THEORY OF THE SPHERING OF RED BLOOD CELLS

Y. C. B. FUNG *and* P. TONG

From the University of California, San Diego, La Jolla, California 92037 and the Massachusetts Institute of Technology, Cambridge, Massachusetts 02139

ABSTRACT A rigorous mathematical solution of the sphering of a red blood cell is obtained under the assumptions that the red cell is a fluid-filled shell and that it can swell into a perfect sphere in an appropriate hypotonic medium. The solution is valid for finite strain of the cell membrane provided that the membrane is isotropic, elastic and incompressible. The most general nonlinear elastic stress-strain law for the membrane in a state of generalized plane stress is used. A necessary condition for a red cell to be able to sphere is that its extensional stiffness follow a specific distribution over the membrane. This distribution is strongly influenced by the surface tension in the cell membrane. A unique relation exists between the extensional stiffness, pressure differential, surface tension, and the ratio of the radius of the sphere to that of the undeformed red cell. The functional dependence of this stiffness distribution on various physical parameters is presented. A critique of some current literature on red cell mechanics is presented.

INTRODUCTION

In an earlier article on the theoretical considerations of the elasticity of the red blood cells (4), it is shown that the assumption that the substance in the interior of the red blood cell be in the liquid state (which cannot sustain shear stress without flow) leads to a number of predictions in agreement with observed features of the red cells. These predictions are based on the biconcave geometrical shape of the red cell and the thinness of the cell wall (with a radius of order 4 μ and a cell wall thickness of order 100 A, and hence a radius-to-thickness ratio of 400). The red cell geometry implies that at the equilibrium state the pressure differential across the cell wall is extremely small, that the cell wall can be deformed into an infinite number of "applicable" (isometric) surfaces without tearing or stretching and without change of the enclosed volume (isochoric); consequently the red cell is capable of large deformation without inducing membrane stresses. These conclusions are independent of the stress-strain law of the cell wall as long as it is elastic, and are valid whatever the thickness distribution of the cell wall may be. The biconcave shape of the red blood cell therefore implies a constant pressure environ-

ment for the hemoglobin, a great flexibility of the cell as an entity, and a freedom from membrane stresses in large deformation under normal circumstances. It clearly relegates any stressing of the cell wall to the action of finite change in volume due to osmosis, and to the shear stresses which occur when the red cell rubs against a vascular wall, or when the shear gradient of flow is large in the cellular dimension.

To inquire into further details of the red cell mechanics, it is necessary to know the stress-strain law of the cell wall, and the wall thickness distribution. For example, in order to calculate the tolerable limits of pressure differential within which the biconcave geometry can be maintained without crenation, we need to know the elastic modulus and the wall thickness. The same information is needed to compute the shear and bending stresses to which the cell wall is subjected in the capillary bed.

It is obvious that the direct measurement of the thickness distribution and the stress-strain law of the red cell wall is extremely difficult. However, it is relatively easy to observe the geometric changes of the red cell when it is placed in a hypotonic solution. Therefore, it is of interest to deduce the implications of overall geometric changes with hypotonicity. One of such changes is the sphering. It is the purpose of the present article to present an analysis of the sphering of the red cell. Our objective is to obtain some insight into the law of elasticity obeyed by the cell wall, or the distribution of thickness of the wall.

Experimental determination of the geometry of the red cell has a particular difficulty in that the dimension of the red cell is so small that the diffraction of visible light over the three-dimensional object is significant under a light microscope. On the other hand, an electron microscope cannot observe a living cell and its change in shape in response to external disturbances. To obtain reliable numerical information a method of numerical processing of the photographic plate is promising; however, it still awaits development.

THE PHENOMENON OF SPHERING

When a red blood cell is placed in a hypotonic solution, it swells to the extent that the osmotic pressure is balanced by the elastic stresses in cell membrane and any changes in surface tension. Returning the cell to an isotonic solution recovers the geometry, so that the transformation seems to be elastic between the initial and the final states. We shall analyze final states of the swelling; hence the cell membrane is assumed to be elastic. The cell contents shall be assumed to be in the liquid state. Whether the red cell behaves viscoelastically during the transient phase of the sphering process is irrelevant to the present study since we shall consider only the states of static equilibrium.

Under the microscope the red blood cells appear to be able to swell into spherical shape in hypotonic solution. It is conceivable that the red cell may become a true sphere. Many observers insisted that this is the case, although accurate documentation remains to be done. Although whether true sphering really happens or not

remains to be seen, theoretical simplicity of the spherical form is so great that a special treatment is warranted.

Consider a relaxed red blood cell which is a body of revolution whose meridional dimensions are shown in Fig. 1. Let this cell be deformed under a uniform internal pressure into a sphere of radius a. Since we shall consider only symmetric deformations, the geometry of the shell is specified completely by a meridian. A point P on the original shell is moved to a point Q on the deformed shell. The point P on the meridian of the original shell may be located by the coordinate pairs S and Φ,

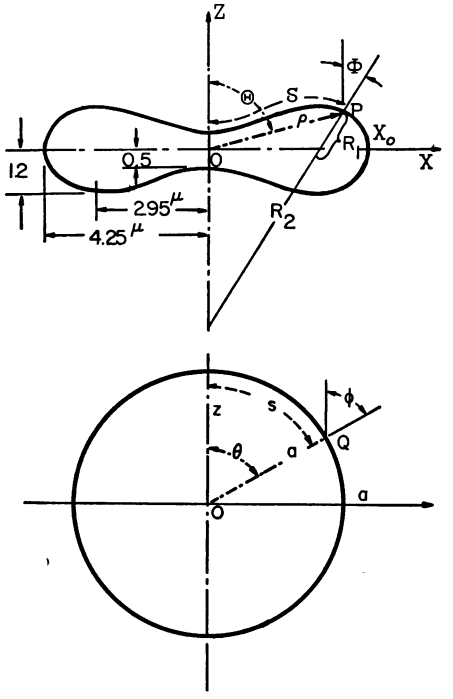

FIGURE 1 Meridonal cross section of (*a*) normal biconcave red blood cell, and (*b*) a sphered red blood cell. Capital letters S, Φ refer to curvilinear coordinates on the normal red cell; the lower case letters s, φ refer to the sphered red cell. Polar coordiuates are ρ, Θ, and a, θ, respectively, for the normal and sphered cells. Z and z are axes of symmetry. Equatorial radius of normal red cell is X_0, that of sphered red cell is a.

X and Z, or ρ and Θ (see Figs. 1 *a* and 1 *b*). The corresponding point Q on the deformed shell can be specified by s and φ, x and z, or a and θ. Here S is the arc length measured along the meridian from the pole to P, Φ is the angle between the normal to the shell at P and the axis of symmetry, and ρ and Θ are the plane polar coordinates as shown in Fig. 1. The equation for the meridional curve (of the original shell) can be expressed by the functions $S = \tilde{S}(\Phi)$, $\rho = \tilde{\rho}(\Theta)$, etc., that of the deformed shell by $s = \tilde{s}(\varphi)$. The deformation is completely described if we know the transformations Θ to θ, ρ to a, or S to s.

The stresses in the shell can be represented by the stress resultants (the so-called membrane stresses) and the stress moments (the bending stresses).[1] We shall ignore

[1] The stress resultants are defined as follows. Consider a thin shell. The geometry of the shell is defined by its middle surface. The spirit of the theory of thin shell is to reduce the analysis of the three-dimen-

the stress moments,[2] and limit our attention to static equilibrium under uniform internal pressure caused by osmosis. The stress resultants are shown in Fig. 2. The equations of equilibrium are[3]

$$\frac{\partial}{\partial S}(rN_s) - N_t \cos\varphi = 0, \quad (r = r_2 \sin\varphi) \tag{1}$$

$$\frac{N_s}{r_1} + \frac{N_t}{r_2} = p \tag{2}$$

where r_1, r_2 are the principal radii of curvature of the deformed shell. See Fig. 1 and the table of notations.

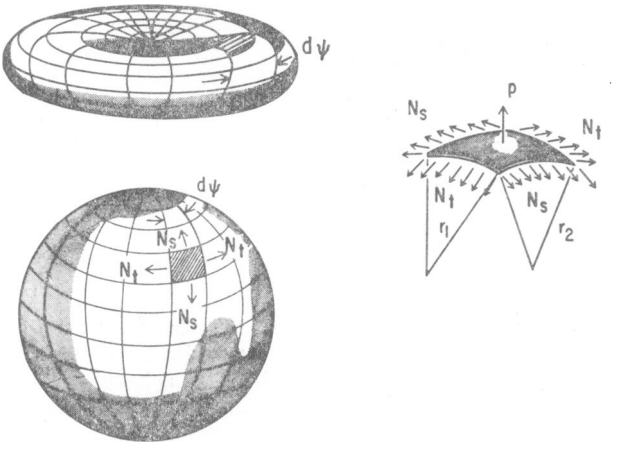

FIGURE 2 Notations for stress resultants N_s, N_t acting in sections passing through the lines of principal curvature with radii of curvature r_1, r_2 respectively.

If the deformed shell is a sphere of radius a,

$$r_1 = r_2 = a \tag{3}$$

---

sional body into that of a two-dimensional curved surface, namely, the middle surface. Draw a curve on the middle surface. Pass a plane tangent to this curve and normal to the middle surface. Across this plane the two sides of the shell interact. This interaction is equivalent to a force and a moment. The force per unit length of the cross section on the mid-surface is called the traction. The traction, being a force, has three components which are called the stress resultants. Two of these lie in the plane tangent to the mid-surface. These are the normal and the shear components, and are often called membrane stresses. The third, perpendicular to the shell mid-surface, is called the transverse shear. Now if the curve named above is a meridian of a surface of revolution, as illustrated in Fig. 2, then we denote the normal stress resultant as N_t, and the shear as N_{ts}. If the curve is a parallel, then the corresponding normal stress resultant is denoted by N_s and the shear, N_{st}. For thin shells it can be shown that $N_{st} = N_{ts}$. For a symmetrically loaded surface of revolution, as is considered in the present paper, both N_{st} and N_{ts} vanish. Therefore we are left with only N_s, N_t in the equations of equilibrium (1) and (2).

[2] The justification is discussed in Appendix C.

[3] See reference 2, p. 22, with $p_s = p_t = N_{ts} = 0$, $p_r = p$.

the unique solution of Equations 1 and 2 is

$$N_s = N_t = \frac{pa}{2}. \tag{4}$$

This simple result holds no matter how the spherical configuration is arrived at. It is the consequence of the spherical geometry.

This tells us at once that being able to sphere is a very special property. An arbitrary shell cannot become a sphere under internal pressure. A shell with a shape shown in Fig. 1 *a* can be transformed into a sphere at a certain pressure only if its elasticity and wall thickness follow certain special laws.

To deduce these laws, let us first compute the strain. In the meridional direction

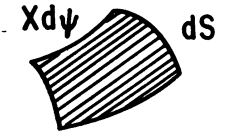

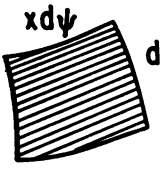

FIGURE 3 Notations for the extension ratios $\lambda_1 = ds/dS$ $\lambda_2 = x(s)/X(S)$. The upper element belongs to the normal relaxed red cell. The lower element belongs to the strained, deformed cell. The extension ratios are formed by dividing the lengths of the corresponding edges.

the extension ratio is obviously ds/dS. In the latitudinal direction it is equal to the ratio of the circumferences and hence the ratio of the radii (see Fig. 3). These extension ratios will be denoted by

$$\lambda_1 = \frac{ds}{dS}, \quad \lambda_2 = \frac{x(s)}{X(S)}. \tag{5}$$

The strain components may be defined in various ways. If Eulerian (Cauchy or Almansi) strains are used, we have

$$e_s = \tfrac{1}{2}[1 - \lambda_1^{-2}], \qquad e_t = \tfrac{1}{2}[1 - \lambda_2^{-2}]. \tag{6}$$

On the other hand, the Lagrangian (Green) strains are defined as

$$e_s = \tfrac{1}{2}[\lambda_1^2 - 1], \qquad e_t = \tfrac{1}{2}[\lambda_2^2 - 1]. \tag{7}$$

The former are based on the metric of the deformed shell. The latter are based on the

metric of the original shell. For a finite deformation it is necessary to make these distinctions.[4]

The elasticity of the shell wall shall be assumed to be nonlinear, isotropic, not necessarily homogeneous, and shall be specified by the following:

$$N_s^{(e)} = \frac{hE}{1 - \nu^2}(e_s + \nu e_t) \tag{8 a}$$

$$N_t^{(e)} = \frac{hE}{1 - \nu^2}(e_t + \nu e_s) \tag{8 b}$$

where E is the Young's modulus, and is a function of the strain invariants:

$$E = E(e_t + e_s , e_t e_s ; \Theta). \tag{9}$$

ν is another elastic constant which also can be a function of the strain invariants.

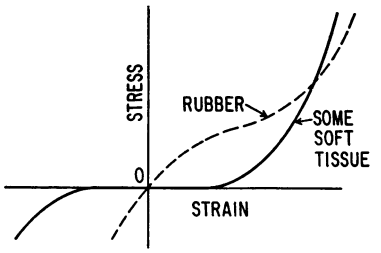

FIGURE 4 Possible nonlinear stress-strain relationships.

The symbol h denotes the wall thickness of the deformed shell. This, in general, is a nonlinear stress-strain law. The values of E and ν depend, of course, on whether e_s , e_t are based on Eulerian or Lagrangian definitions. The justification of Equation 8 is discussed in Appendix A. A general sketch is shown in Fig. 4.

The tension in the membrane consists of two parts: the elastic stress resultant and the surface tension. Surface tension (force per unit length or surface energy per unit area) exists on both sides of the cell membrane. Because the nature of the membrane, as well as the fluids that come into contact with it, may be different on the two sides of the membrane, we should have two different quantities, $\gamma^{(0)}$, $\gamma^{(i)}$, to represent the surface tension on the outside and inside of the cell membrane, respectively. However, only the resultant γ,

$$\gamma = \gamma^{(i)} + \gamma^{(0)} \tag{10}$$

is of importance in the mechanics of sphering when the stress-moments are ignored Let the membrane stress in the deformed cell be written as

$$N_s = N_s^{(e)} + \gamma, \qquad N_t = N_t^{(e)} + \gamma \tag{11}$$

[4] See reference 5, pp. 89–99 and reference 7.

where $N_s^{(e)}$ and $N_t^{(e)}$ are the elastic stresses which correspond with the strains e_s, e_t measured from a natural state, and are given by Equation 8. We further assume that the surface tension, as well as the red cell geometry and the elasticity, is symmetrically distributed. Then when the red cell swells into a sphere, the equilibrium condition Equation 4 holds, and we obtain, on solving Equation 8 for e_s, e_t, and applying Equations 4 and 11:

$$e_s = e_t = \frac{1}{Eh}(N_s^{(e)} - \nu N_t^{(e)}) = \frac{1-\nu}{Eh} N_s^{(e)}$$

$$= \frac{1-\nu}{Eh}(N_s - \gamma) = \frac{1-\nu}{Eh}\left(\frac{pa}{2} - \gamma\right). \tag{12}$$

To obtain explicit results we shall use plane polar coordinates (Fig. 1) in which the Eulerian strains of Equation 6 may be written, since

$$ds = a\,d\theta, \qquad dS = \sqrt{\rho^2\,d\Theta^2 + d\rho^2},$$

$$e_s = \frac{1}{2}\left\{1 - \frac{1}{a^2}\frac{\left[\left(\frac{d\rho}{d\Theta}\right)^2 + \rho^2\right]}{\left(\frac{d\theta}{d\Theta}\right)^2}\right\} \tag{13 a}$$

$$e_t = \frac{1}{2}\left\{1 - \frac{\rho^2 \sin^2\Theta}{a^2 \sin^2\theta}\right\}. \tag{13 b}$$

Equating 13 *a* and 13 *b* according to Equation 12, we obtain

$$\frac{1}{\rho^2}\left(\frac{d\rho}{d\Theta}\right)^2 + 1 = \frac{\sin^2\Theta}{\sin^2\theta}\left(\frac{d\theta}{d\Theta}\right)^2 \tag{14 a}$$

or

$$\frac{d\theta}{\sin\theta} = \left[1 + \frac{1}{\rho^2}\left(\frac{d\rho}{d\Theta}\right)^2\right]^{1/2}\frac{d\Theta}{\sin\Theta}, \qquad \left(0 \leqq \Theta \leqq \frac{\pi}{2}\right). \tag{14 b}$$

An integration gives the basic transformation

$$\tan\frac{\theta}{2} = \exp\left\{-\int_\Theta^{\pi/2}\left[1 + \frac{1}{\rho^2}\left(\frac{d\rho}{d\Theta}\right)^2\right]^{1/2}\frac{d\Theta}{\sin\Theta}\right\} \tag{15}$$

where the integration constant has been determined by the condition of symmetry, i.e., that $\theta = \pi/2$ when $\Theta = \pi/2$. It is interesting to note that this transformation is independent of the elastic moduli, wall thickness, surface tension, and the radius of the sphere a. It follows purely the requirement that for a spherical

membrane in static equilibrium under internal pressure the principal strains e_t and e_s must be equal.

Equating 13 *b* and 12 yields the other basic relationship

$$\frac{1-\nu}{Eh}\left(\frac{pa}{2}-\gamma\right)=e_t=\frac{1}{2}\left[1-\frac{\rho^2\sin^2\Theta}{a^2\sin^2\theta}\right] \tag{16}$$

where

$$\sin^2\theta=4\tan^2\frac{\theta}{2}\Big/\left(1+\tan^2\frac{\theta}{2}\right)^2 \tag{17}$$

can be computed from Equation 15. When the red cell shape is specified, the right hand sides of Equations 15 and 16 are known.

Therefore, sphering is possible if the function $(1-\nu)\ (pa-2\nu)/(2Eh)$ follows a particular variation along the meridian as specified by Equation 16.

Before examining Equation 16 numerically, let us add two formulas. If the elasticity law Equation 8 is based on the Lagrangian strain, the corresponding result for $\tan\frac{\theta}{2}$ is the same as Equation 15, whereas in place of Equation 16 we now have

$$\frac{1-\nu}{Eh}\left(\frac{pa}{2}-\gamma\right)=\frac{1}{2}\left[\frac{a^2\sin^2\theta}{\rho^2\sin^2\Theta}-1\right]. \tag{18}$$

If the red cell shape is specified in X, Z coordinates, we have, in place of Equation 15,[5]

[5] For practical calculations it is desirable to remove the singularities in the integrals in Equations 15 and 19. To remove the singularity at the lower limit, as $\Theta\to 0$ and $X\to 0$, we subtract and add 1 to the numerators of the integrands in Equations 15 and 19, integrate the last term explicitly, and reduce the results to obtain

$$\tan\frac{\theta}{2}=\tan\frac{\Theta}{2}\exp\left\{-\int_\Theta^{\pi/2}\frac{\left[1+\frac{1}{\rho^2}\left(\frac{d\rho}{d\Theta}\right)^2\right]^{1/2}-1}{\sin\Theta}\,d\Theta\right\} \tag{15 a}$$

$$\tan\frac{\theta}{2}=\frac{X}{X_0}\exp\left\{-\int_X^{X_0}\frac{\left[1+\left(\frac{dZ}{dX}\right)^2\right]^{1/2}-1}{X}\,dX\right\}. \tag{19 a}$$

The integral in Equation 15 *a* is regular. That in Equation 19 *a*, however, has a singularity at the upper limit since $dZ/dX\to\infty$ at X_0, because the cell wall has a vertical tangent there on account of the symmetry with respect to the equatorial plane and the continuity of the slope. To remove the difficulty, we can take Z as the independent variable so that

$$\tan\frac{\theta}{2}=\exp\left\{-\int_Z^0\left[\left(\frac{dX}{dZ}\right)^2+1\right]^{1/2}\frac{dZ}{X(Z)}\right\}. \tag{19 b}$$

In practice, we use Equation 19 *a* for $0\le X\le 0.98\,X_0$, and Equation 19 *b* for $0.98\,X_0\le X\le X_0$.

$$\tan\frac{\theta}{2} = \exp\left\{ -\int_{X}^{X_0}\left[1+\left(\frac{dZ}{dX}\right)^2\right]^{1/2}\frac{dX}{X}\right\} \tag{19}$$

where X_0 is the equatorial radius of the red cell. In X, Z coordinates, $\rho \sin \Theta$ in Equation 16 is X.

DISTRIBUTION OF THE EXTENSIONAL STIFFNESS OF THE CELL WALL

We see that the ability of a red cell to sphere requires that the parameter $(1 - \nu)(pa - 2\gamma)/(2Eh)$ satisfy Equation 16. This parameter depends on the product of E and h, both of which may vary along the meridian. We shall call the product Eh the "extensional stiffness" of the membrane.

If the red cell wall is homogeneous and linearly elastic, then E, ν, and γ are constants and the extensional stiffness can be a function of Θ satisfying Equation 16

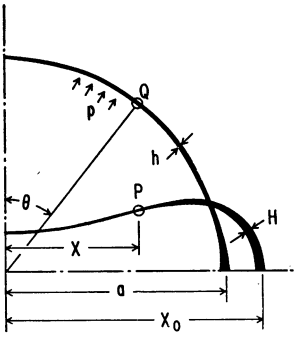

FIGURE 5 Schematic drawing showing variable extensional stiffness. Distributions $Eh(x)$ and $EH(X)$ in the sphered red cell and the normal biconcave red cell, respectively. E is the Young's modulus in the strained state; h is the wall thickness in the strained state; H is the wall thickness in the relaxed state.

only if the thickness variation h is inversely proportional to the right hand side of Equation 16. We note that h is the wall thickness of the deformed shell, which varies, of course, with the strain. In finite deformation such a strain-dependent variation must be taken into account. Furthermore, if the elasticity of the red cell wall is nonhomogeneous, then E and ν vary spatially; if the wall elasticity is nonlinear, then E, ν are functions of e_s, e_t.

Let us consider the thickness variation which will be denoted by $h(\theta)$ and $H(\Theta)$ for the sphered and the relaxed red cell, respectively (Fig. 5). $H(\Theta)$ can be computed from $h(\theta)$ if we know the strain and if we know the compressibility of the material. Let us assume that the material is incompressible, which can be specified (exactly in infinitesimal strains but approximately in finite strains) by setting the Poisson's ratio ν to be $\frac{1}{2}$. Consider the change of volume of a portion of the sphered red cell in the form of a narrow circular ring bounded between two neighboring parallel circles at θ and $\theta + d\theta$. The thickness of the ring being h, the width being $ds = a\,d\theta$, and the circumference being $2\pi a \sin\theta$, then the volume of the ring is $2\pi a^2 h \sin\theta\, d\theta$. The corresponding ring in the relaxed cell has thickness H, length

$2\pi\rho \sin \Theta$, and width dS:

$$dS = \left[\rho^2 + \left(\frac{d\rho}{d\Theta}\right)^2\right]^{1/2} d\Theta,$$

hence the volume $2\pi\rho H\, dS \sin \Theta$. Equating these volumes on account of the incompressibility, we obtain

$$a^2 h \sin \theta\, d\theta = \rho^2 H \sin \Theta \left[1 + \frac{1}{\rho^2}\left(\frac{d\rho}{d\Theta}\right)^2\right]^{1/2} d\Theta.$$

Hence

$$H = h \frac{a^2 \sin \theta}{\rho^2 \sin \Theta}\left[1 + \frac{1}{\rho^2}\left(\frac{d\rho}{d\Theta}\right)^2\right]^{-1/2} \frac{d\theta}{d\Theta}. \tag{20}$$

A substitution of $d\theta/d\Theta$ from Equation (14 *b*) gives finally

$$H = h \frac{a^2 \sin^2 \theta}{\rho^2 \sin^2 \Theta}. \tag{21}$$

We notice that the parameter

$$B = \frac{a^2 \sin^2 \theta}{\rho^2 \sin^2 \Theta} \tag{22}$$

appears frequently. B can be computed from Equations 17 and 18 or 19. Let the values of Eh from Equation 16 (using Eulerian strain) and from Equation 18 (using Green's strain) be distinguished by the superscripts E and G respectively; and similarly for EH, then

$$EH^{(E)} = Eh^{(E)}B = EH^{(G)}B = Eh^{(G)}B^2. \tag{23}$$

We are now ready to examine some numerical examples. For the convenience of computation, we shall choose the unit of length so that $X_0 = 1$. Since Equations 15–19 and 22, 23 are all in dimensionless form, such a choice of scale means only that we divide all the initial cell dimensions in micra by X_0 in micra. Lacking detailed information about the red cell geometry, we shall assume that the meridional section in the undeformed state can be expressed by a polynomial equation. Since the equation must be symmetric in $+Z$ and $-Z$, and in $+X$ and $-X$, as the red cell is symmetric with respect to the polar axis and the equatorial plane, the equation must contain only even powers of Z and X. Thus we assume

$$Z^2 = (1 - X^2)(C_0 + C_1X^2 + C_2X^4). \tag{24}$$

The first factor on the right hand side is dictated by the condition $Z = 0$ when

$X = \pm 1$. If we choose C_0, C_1, C_2 to fit Ponder's data (14, 15) on the red cell diameter, and the locations and values of the maxima and minima of the cell as shown in Fig. 1, we have

$$C_0 = 0.01384083, \qquad C_1 = 0.2842917, \qquad C_2 = 0.01306932.$$

Then the cell shape as given by Equation 24 is plotted in Fig. 1. The large number of digits quoted for these constants does not mean that the cell shape is known to such accuracy, but they are kept to avoid purely numerical rounding-off errors in

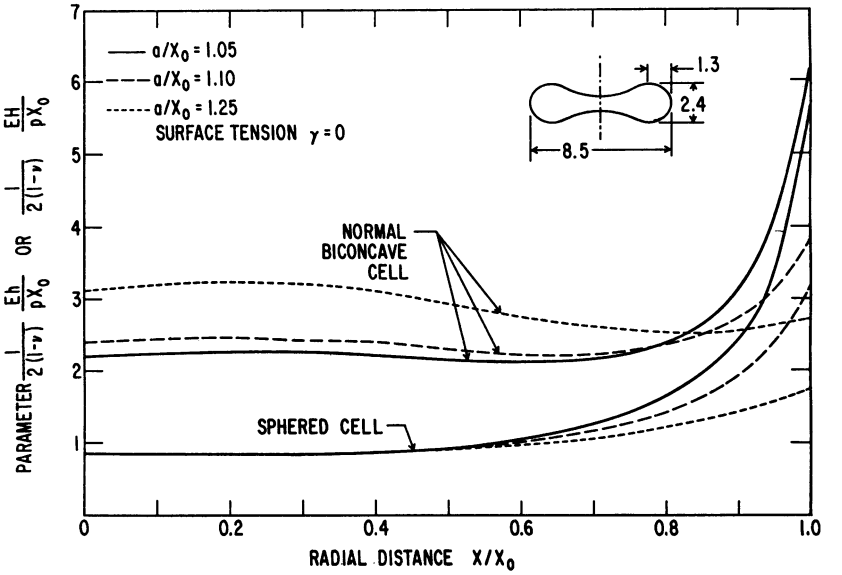

FIGURE 6 The distribution of the extensional stiffness of the red cell wall plotted as a function of the radial coordinates. Because different areas of the red cell are stretched differently during the sphering process, the thickness distribution is different in the two configurations. Surface tension γ is taken to be zero for this figure.

the computational process. The final result is to be accepted with no more than one or two significant figures accuracy.

As a useful check on the numerical calculations, we note that as $X \to 1$, $\sin^2 \Theta$ and $\sin^2 \theta$ tend to 1 and Equation 16 yields the limiting value

$$\left(\frac{1-\nu}{Eh}\right)\left(\frac{pa}{2} - \gamma\right)_{X=1} = \frac{a^2 - 1}{2a^2}. \tag{25}$$

Since X_0 is taken to be 1, a in this formula is the ratio of the radius of the sphere to X_0.

To discuss the numerical results, we shall consider first the case of zero surface

tension. Numerical integration of Equation 19 and others leads to the results as shown in Fig. 6 in case the surface tension is zero. Here the original extensional stiffness distribution of the cell wall, $2EH/(1 - \nu)$, is plotted as a function of the radial distance X/X_0. We see that the extensional stiffness of the cell wall is not uniform for those biconcave cells that can sphere. The stiffness variation depends on the ratio of the diameter of the sphere to the diameter of the undeformed red cell, a/X_0. If the ratio a/X_0 is very close to 1, a very large local stiffening at the equator is needed. If the radius of the sphere is only one per cent larger than the undeformed cell ($a/X_0 = 1.05$), the stiffness at the equator would have to be 12.4 times the stiffness at the pole (data for this case was not plotted in Fig. 6). If the radius of the sphere is 5 per cent larger than the undeformed cell, ($a/X_0 = 1.05$), then the

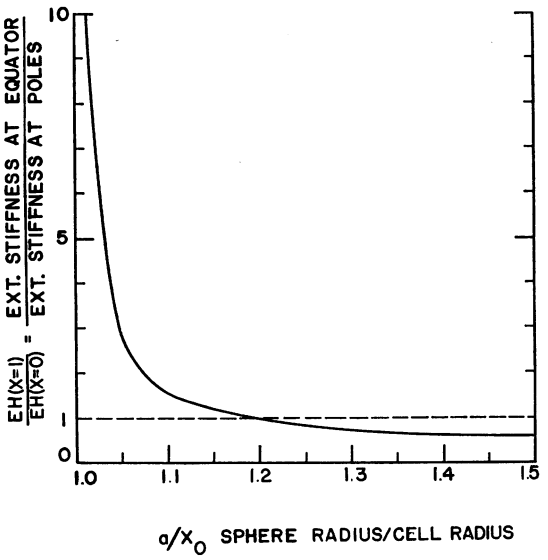

FIGURE 7 The necessary ratio of the extensional stiffness at the equator to that at the poles in order that a normal biconcave red cell of radius X_0 be able to become a sphere of radius a in a hypotonic solution. The surface tension γ is taken to be zero for this figure. Only when the surface tension γ is nonvanishing and variable over the surface can a biconcave red cell be transformed into a sphere with radius a smaller than X_0 in a hypotonic solution.

equatorial stiffness is required to be 2.76 times that at the poles. This raio decreases as the ratio a/X_0 increases, until at $a/X_0 = 1.19$ the trend is reversed. See Fig. 7. For larger spheres the location of the most stiff point is somewhere near the axis of symmetry. A similar plot of the stiffness distribution in the sphered cell is shown in the same Fig. 6.

Since we do not know the red cell geometry accurately, it is expedient to examine the variations in the solution with a whole class of cell shapes. Numerically this is very easy to do. One just varies the constants C_0, C_1, and C_2 in some systematic way. A set of such calculations shows, for example, that the stiffness distribution is quite insensitive to the location of the maximum thickness of the red cell. If this location is shifted closer to the axis of symmetry by 10 per cent of cell radius, the maximum change in EH is no more than 5 per cent when $a/X_0 = 1.05$. Variation of

other parameters produced similar insignificant results. These results are not presented because when accurate geometric measurements are obtained in the future, a repetition of the numerical calculations can be done very quickly.

Next, let us consider the effect of surface tension γ. The possibility of a variable surface tension distribution $\gamma(\Theta)$ permits us to consider negative strain $e_s = e_t$. Fig. 8 shows the distribution of e_s, and hence of

$$\frac{1-\nu}{Eh}\left(\frac{pa}{2}-\gamma\right)$$

over a meridional section of the red cell.[6] Note that this parameter can be negative when $a/X_0 < 1$. Since p is a constant, and $Eh/(1-\nu)$ has to be positive to have a physical significance, we see that such a change of sign of e_s can happen only if γ is smaller than $pa/2$ when X is small and greater than $pa/2$ when X is large. Therefore we conclude that *if the radius of the sphered red blood cell is smaller than that of the normal red cell, then the surface tension would have to be greater at the equator than at the poles (i.e., the dimples).*

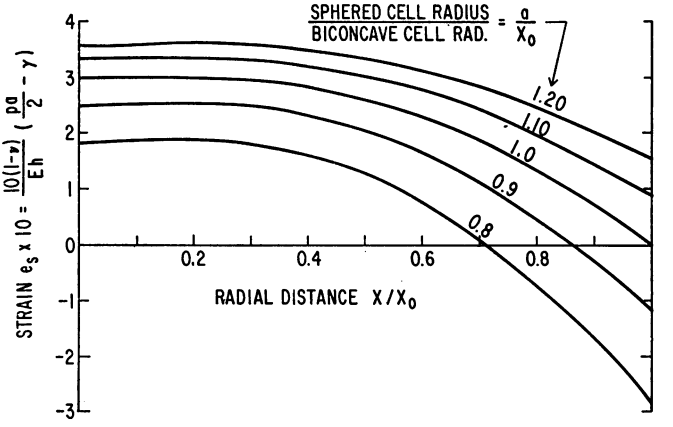

FIGURE 8 The radial distribution of the Eulerian strain $e_s = e_t$ in the sphered red blood cell. The strain e_s is equal to the parameter $\frac{(1-\nu)}{Eh}\left(\frac{pa}{2}-\gamma\right)$; hence this figure shows also the necessary distribution of the reciprocal of the extensional stiffness of the wall as related to the surface tension.

Ponder (15) suggested that the surface area remains constant in sphering. If this were the case, then $a = 0.8155$ for a red cell geometry specified by Equation 24. We must note that a common belief that the cell membrane must be inextensible if the total area remains constant is erroneous. An inextensible biconcave shell

[6] The radius X_0 in Fig. 8 refers to that of the *relaxed* (unstressed) biconcave shell. If the surface tension is variable and $\neq 0$ over the cell membrane in the normal condition, it is necessary to calculate the relaxed configuration from the observed geometry and γ distribution.

cannot sphere. Local extension is necessary for sphering. This is due to the fact that no sphere can be isometric with a biconcave shell.

The surface tension γ between the red cell membrane and the plasma on the one side and the hemoglobin on the other has not been measured. The present theory provides a relation between γ and the sphering radius. If the sphered red cell radius is smaller than the equatorial radius of the unstrained red cell, then $\gamma = pa/2$ at the point where $e_s = 0$. If p turns out to be of the order of 2.3 mm H_2O as stated by Rand and Burton (18), then for $a \doteq 4 \times 10^{-4}$ cm we have $\gamma \doteq 5 \times 10^{-4}$ dyne/cm, which is five orders of magnitude smaller than that of the water and air interface.

For a red cell to be transformed into a perfect sphere, not only is the parameter $(1 - \nu)\ (pa - 2\gamma)/(2\ Eh)$ required to have the right variation over the cell, it must also satisfy the specific numerical value shown in these figures. Hence the product pa is fully determined in each case. The internal pressure p is determined by the chemical potential. At equilibrium when there is no mass transfer across the cell membrane the osmotic pressure must balance the hydrostatic pressure p. In other words, a red cell can swell only into a sphere of a specific radius, if it can do so at all.

DISCUSSIONS AND CONJECTURES

The simplicity of the present analysis is truly remarkable. It is achieved through the spherical geometry of the swelled cell. Should it be desired to analyze the swelling of the red cell into an intermediate, ellipsoidal shape, we would have to carry out a step-by-step numerical integration of a set of nonlinear differential equations with variable coefficients. Indeed, we know of few nonlinear problems which can be solved by a method so simple and yet applicable to so general a material and so complex an initial geometry.

However, since the partial differential equations governing the static equilibrium of a thin shell (in the full bending-stretching theory) are of the elliptic type, small deviations in geometry are expected to induce only small changes in the stress and strain. Hence the perturbation method can be applied so that the theory can be modified readily to the case in which the red cell swells into an ovaloid which does not differ too much from a sphere.

The theory is suggestive to the experimenter to look for possible variations in wall thickness, elasticity, and surface tension, and to determine whether true sphering occurs, and if so, at what radius and what internal pressure. However, there are a number of recently discovered facts which may be considered in this connection.

The most important is John Murphy's discovery (13) that the cholesterol in the erythrocytes is concentrated around the equator. Now cholesterol is a relatively stiff material. It attaches to the erythrocyte cell membrane, and might very well be

the cause of a local variation of surface tension and an increased Young's modulus or an increased effective wall thickness. Murphy's theory of surface-tension–controlled biconcave shape, however, appears to be in error and is discussed in Appendix B.

The second fact is that an erythrocyte in a hypotonic solution behaves differently than a rubber model in a similar situation. In reference 4, the author discussed the behavior of a seamless thin-walled latex rubber biconcave shell (radius-to-thickness ratio of order 400) under internal pressure. When this rubber model of the red cell is gradually pressurized, the dimples at the poles first pop out, then buckling occurs along the equator, as shown in Fig. 7 of reference 4. The buckling occurs because as the cell tries to sphere the equator shortens. The number of buckles increases with increasing internal pressure. At a sufficiently high pressure the shell becomes smooth again. However, the rubber model could not sphere, and it failed by aneurism.

When a red cell is observed under the microscope, such buckles cannot be seen. One may hypothesize that the absence of the buckle is due to the non-linear stress-strain relationship of the cell material. If the cell wall behaves in a manner similar to other soft tissues, such as the mesentery, the blood vessels, the skin, the striated and the heart muscles, then an exponential stress-strain relationship is expected (Fig. 4). For such a material Young's modulus approaches zero at zero stress, then it increases linearly with increasing stress, and exponentially with increasing strain. The essence is that the material is very soft in the natural state, much softer than the rubber at the corresponding state. Now the buckling such as shown in the Fig. 7 of reference 4 occurs because at the critical compressive buckling stress the compressive strain of the rubber is not large enough to absorb the required shortening. If the elastic modulus was exponential for the erythrocyte, the critical buckling stress would approach zero, but the strain could be finite, so that wrinkles might be absent.

In a larger scale, a similar situation exists in compressing an artery. Rushmer et al. (11) show that under an external pressure a rubber tube buckles and flattens whereas a femoral artery just shrinks in size but remains round. Undoubtedly in the case of the femoral artery, the stability of the blood vessel is increased by the surrounding tissues, but the ability of the artery to reduce its diameter is marked.

If we take the absence of the buckles to mean that a nonlinear stress-strain law such as the exponential law of the arteries, skin, and muscles is reasonable also for the erythrocyte, then the extreme flexibility of the normal red cells is to be expected. For, in addition to the reasons explained in reference 4, we now add that any secondary stresses (bending and stretching) resisting a change of shape from the normal biconcave shape are very small.

Ponder's (15) classical discussion on the sphering of red cells offers much information. In some details Rand and Burton (18) state that "when equilibrated with a sufficiently hypotonic medium, so that the dimple curvature has been reversed and the cell is a swollen ellipsoid, then the cells very abruptly 'popped' from

the swollen ellipsoid into a perfect 'glassy' sphere." Since an ellipsoid is a stable configuration, this suggests a rapid change in elasticity between the stages of ellipsoid and the sphere, which hints at an exponential law similar to other soft tissues.

Of the great flexibility of the red cell wall there is no doubt. Recent work of Guest et al. (9) shows that the red cell wall can be deformed into cusp-like edges when the cell moves through capillaries of small calibre. Gregerson and his associates (8) report on the passage of washed red cells through circular holes in polycarbonate filters. The red cells can pass through holes less than one third cell diameter without hemolysis and with no driving force other than the cell's own weight. Teitel (21) finds in similar experiments on passing red cells through filter papers that the red cell elasticity (called "plasticity" by Teitel) is influenced critically by heating to 49.5°C.

There are several other puzzling facts related to the red cell wall reported recently: (*a*), Baker's (1) electron microscopic observation on hemolyzing red cells which grow long hairs prolifically, and his capture of the "crowning" of red cells when the cell walls were broken locally when the cells were placed in a hypotonic solution which contained gluteraldehyde for fixation. (*b*), Stewart's (20) electron microscopic observation of the detached membrane and integument in an abrazed red cell. (*c*), Kochen's (10) observation about pulling the cell wall into a filament when the cell adheres to a glass surface at a single point. In a speculative vein these facts taken together suggest that the red cell wall may not be a bimolecular layer of lipids. It is hard to conceive that such a bimolecular layer would have the great extensibility and exponential stiffening that is desired. As an alternative one might suggest that the molecules are arranged in some kind of layered spirals which uncoil under various stresses. Perhaps the uncoiling may provide the key to the elastic stiffening, the filament and the hair formation, and the integument appearance in the process of hemolysis of the red cells.

CONCLUSIONS

By assuming that the red blood cell is a fluid-filled shell and that it can swell into a perfect sphere in an appropriate hypotonic medium, we obtain a rigorous solution of the sphering transformation. The solution presented in this paper is valid for finite strains of the red cell membrane, under the most general nonlinear elastic stress-strain law for an isotropic, incompressible material in a state of generalized plane stress. The surface tension variation is taken into account.

A necessary condition for a red cell to be able to sphere is that the surface tension and the extensional stiffness follow specific distributions over the membrane. If the surface tension distribution and the ratio of the radius of the sphere to that of the undeformed red cell are known, then this extensional stiffness distribution is determined. Therefore, the measurement of sphering would provide important information about the mechanical property of the red cell membrane.

This work is supported by the United States Air Force Office of Scientific Research under grant No. 1186-67 and the National Science Foundation under grant No. GK-1415.
Dr. Fung is Professor of Bioengineering and Applied Mechanics, Department of Aerospace and Mechanical Engineering Sciences, Revelle College and Medical School, University of California, San Diego. Dr. Tong holds a Ph.D. and is Assistant Professor in the Department of Aeronautical and Astronautical Engineering, Massachusetts Institute of Technology.

Received for publication 14 September 1967.

APPENDIX A

Justification of the Stress-Strain Law–Equation 8

We shall show that the formulation of the stress-strain law presented in Equation 8 is the most general one for a two-dimensional generalized plane-stress field in an isotropic incompressible material under the general assumption that the stress is an analytic function of the strain. That Equation 8, which is formally similar to the familiar linear elasticity law, is indeed the most general one in nonlinear finite deformation under a very broad assumption, is a fact that does not seem to have been pointed out before. The corresponding result valid for a three-dimensional field was presented earlier by Prager (16). But the two-dimensional result is very much simpler. In three-dimensional fields, the analogy with the linear elasticity formula is not valid.

Let us consider a thin membrane stressed by forces acting in the plane of the membrane while the forces acting on the faces of the membrane are so small that the stresses normal and tangential to the membrane surface are negligibly small compared with the stresses in the plane of the membrane. This is the so-called plane state-of-stress. The state of strain corresponding to a plane state-of-stress is in general not plane; the thickness of the membrane will vary with the stress. However, if the material is incompressible, then the strain normal to the membrane is determined entirely by the strain in the plane of the membrane. Hence in the state so specified the state of stress and strain can be described by the matrices

$$\mathfrak{d} = \begin{pmatrix} \sigma_x & \sigma_{xy} \\ \sigma_{xy} & \sigma_y \end{pmatrix}, \qquad \mathbf{e} = \begin{pmatrix} e_x & e_{xy} \\ e_{xy} & e_y \end{pmatrix} \tag{A. 1}$$

where x, y are orthogonal coordinates in the plane of the membrane.

We assume that the material is isotropic and that the stress is an analytic function of the strain. This means that the stress is expressible as a power series of the strain. Thus

$$\mathfrak{d} = c_0\mathbf{I} + c_1\mathbf{e} + c_2\mathbf{e}^2 + c_3\mathbf{e}^3 + \cdots \tag{A. 2}$$

where c_0, c_1, c_2 $\cdots$ are constants. The characteristic equation of $\mathbf{e}$ is

$$0 = |\mathbf{e} - \lambda\mathbf{I}| = \begin{vmatrix} e_x - \lambda & e_{xy} \\ e_{xy} & e_y - \lambda \end{vmatrix} \tag{A. 3}$$

i.e.,

$$\lambda^2 - (e_x + e_y)\lambda + (e_xe_y - e_{xy}) = 0. \tag{A. 3 a}$$

Let the roots of this equation be e_1 and e_2. Then e_1, e_2 are the principal strains which are

invariant with respect to rotation of coordinates. From Equation (A. 3 *a*) we have

$$e_1 + e_2 = e_x + e_y, \qquad e_1 e_2 = e_x e_y - e_{xy}^2 \cdot \tag{A.4}$$

Writing α, β for the first and second invariants of strain,

$$\alpha = e_1 + e_2, \qquad \beta = e_1 e_2 \tag{A. 5}$$

we have

$$\lambda^2 - \alpha\lambda + \beta = 0. \tag{A. 6}$$

According to Cayley-Hamilton's theorem (12), a matrix satisfies its own characteristic equation. Hence we have the matrix equation

$$\mathbf{e}^2 - \alpha\mathbf{e} + \beta\mathbf{I} = 0 \tag{A. 7}$$

where I is the idemfactor. Multiply Equation A. 7 successively by $\boldsymbol{e}$, $\boldsymbol{e}^2$, $\boldsymbol{e}^3 \cdots$ and solve for the highest power, we obtain

$$\begin{aligned} \mathbf{e}^2 &= \alpha\mathbf{e} - \beta\mathbf{I} \\ \mathbf{e}^3 &= (\alpha^2 - \beta)\mathbf{e} - \alpha\beta\mathbf{I} \\ \mathbf{e}^4 &= [\alpha(\alpha^2 - \beta) - \alpha\beta]\mathbf{e} - (\alpha^2 - \beta)\beta\mathbf{I} \\ &\cdots\cdots\cdots \end{aligned} \tag{A. 8}$$

On substituting these powers into Equation A.2, collecting terms, and rearranging, we see that the result can be written as

$$\mathbf{\sigma} = \mu(\alpha, \beta)\mathbf{e} + \eta(\alpha, \beta)\mathbf{I} \tag{A. 9}$$

where $\mu(\alpha, \beta)$, $\eta(\alpha, \beta)$ are functions of α and β; i.e., functions of the strain invariants $e_1 + e_2$, $e_1 e_2$. Thus the stress tensor is equal to the sum of one term proportional to the strain tensor and another proportional to an isotropic tensor. If we now write

$$\eta(\alpha, \beta) = \lambda(\alpha, \beta)\alpha, \tag{A. 10}$$

which in general should be permissible unless $\alpha = 0$, (in an infinitesimal strain field, incompressibility implies $e_1 + e_2 + e_3 = 0$, so that in general $e_3 = -(e_1 + e_2) \neq 0$), then Equation A.9 becomes

$$\mathbf{\sigma} = \mu(\alpha, \beta)\mathbf{e} + \lambda(\alpha, \beta)(e_x + e_y)\mathbf{I}. \tag{A. 11}$$

The last equation is identical in form to the linear elasticity law. The functions $\mu(\alpha, \beta)$, $\lambda(\alpha, \beta)$ are the nonlinear analog of the Lamé constants.

Equation A.11 can be reduced to Equation 8 if we identify[7]

[7] See reference 5, p. 129.

$$E = \frac{\mu(3\lambda + 2\mu)}{\lambda + \mu}, \qquad \nu = \frac{\lambda}{2(\lambda + \mu)}$$
$$N_x = h\sigma_x \qquad N_y = h\sigma_y . \tag{A. 12}$$

Thus the validity of our assumed law is verified.

The corresponding result for the three-dimensional field given by Prager (16, 17) referred to above is

$$\mathfrak{d} = \mu_1 \mathbf{e}^2 + \mu_2 \mathbf{e} + \mu_3 \mathbf{I}. \tag{A. 13}$$

Here μ_1, μ_2, and μ_3 are functions of the strain invariants. Since in general we have no right to remove the e^2 term, no analog can be drawn with the linear theory.

A final remark about the assumption of incompressibility. This assumption is not essential. It was introduced merely to justify that the two-dimensional strain tensor e given in Equation A.1 is sufficient to specify completely the strain in a body in a plane-stress state. It can be replaced by knowing the three-dimensional stress-strain law (Equation A.13) so that the normal strain e_z and the shear strains e_{zx}, e_{zy} (z is the axis normal to x and y) can be computed from the two-dimensional strain tensor (Equation A.1) and the conditions of plane stress, $\sigma_z = \sigma_{zx} = \sigma_{zy} = 0$. However, since for soft biological tissues the bulk modulus is several orders of magnitude higher than the shear modulus, the assumption of incompressibility is usually applicable.

APPENDIX B

Critique of Some Theories of the Mechanical Properties of Red Cell Membrane

Many theories of the red cell membrane are based on an analogy with liquid droplets under the action of surface tension. The most recent and prominent are those of Rand and Burton (18) and Murphy (13). Since these theories differ in their fundamental approach from the present paper, it is necessary to discuss the differences.

Murphy (13) discovered that the cholesterol distribution in the red cell is nonuniform, and suggested that the surface tension in the cell membrane is also nonuniform. He then showed that an oil drop on water would produce a concavity in the interface if a local decrease of surface tension was introduced. A drop of Cristo oil floating on water assumed a round shape. A tiny speck of detergent was introduced to touch the bottom of the oil drop, which then changed into a monoconcave shape with the bottom curved upward. Murphy suggests that the biconcave shape of the red cell is obtained by such a mechanism.

There is a basic difficulty in extrapolating the floating oil drop result to a red cell wholly immersed in a fluid. Consider the forces that act on an immersed droplet. For simplicity's sake let us assume that the density of the fluid in the droplet is the same as the external fluid. Then the hydrostatic pressure due to gravity is the same everywhere on both sides of the interface. Therefore the only possible pressure differential that may act on the interface is a uniform internal pressure p_0.

Now consider the floating droplet. The free surface of the water is perpendicular to the gravitational field. If we denote the distance from the free surface by z, then at equilibrium the static pressure inside the droplet is $p_0 + \bar{\rho}gz$, where p_0 is the pressure inside the droplet at the level of the free surface ($z = 0$), $\bar{\rho}$ is the density of the droplet, and g is the gravitational acceleration. If all pressures are stated as gauge values then the pressure in the air

is zero, and that in the liquid outside the droplet is ρgz, where ρ is the density of the water. The pressure distribution acting on the interface may be listed as follows:

	Floating droplet		Immersed droplet
	On upper surface $z = -z_1$	On lower surface $z = z_2$	On entire surface
In droplet	$p_0 - \bar{\rho}gz_1$	$p_0 + \bar{\rho}gz_2$	$p_0 + \rho gz$
Outside droplet	0	ρgz_2	ρgz
Differential	$p_0 - \bar{\rho}gz_1$	$p_0 + (\bar{\rho} - \rho)gz_2$	p_0

The pressure differential listed in the last line is what must be balanced by the surface tension and curvature of the interface. Since z_1, z_2 are variable over the droplet, the dissimilar nature between the floating droplet and the immersed one is evident.

Although we have shown that the floating droplet is not a reliable model for the red cell, we did not say that surface tension is not an important factor in determining the red cell geometry. In fact, the analysis presented in reference 4, as well as the present paper, argues for the extreme importance of surface tension. The sphering or antisphering agents probably act through the control of surface tension. In this connection we observe that the introduction of hypotonicity by adding water to the medium not only affects the osmosis, but also increases the surface tension between the cell membrane and the solution. The final osmotic pressure across the cell wall is balanced by the resultant of the elastic stress and the surface tension. Following the analysis of reference (4), we conclude that if the red cell shape is biconcave then at equilibrium the resultant of the surface tension and the elastic stress must approach zero.

Next we shall discuss the work of Rand and Burton (18), who described an interesting experiment on sucking red cell membranes into small pipettes. Among other things they concluded: (*a*) There is no difference in stiffness between the rim and the biconcavity of the red cell or between biconcave discs and hypotonically swollen (not sphered) cells. (*b*) Normal and swollen cells showed a pressure gradient of 2.3 $\pm$ 0.8 (SE) mm H_2O. If these conclusions were established rigorously, they would settle many questions about red-cell mechanics. Unfortunately, these conclusions were arrived at after the addition of several unwarranted assumptions which will be discussed below.

Rand and Burton's (18) initial hypothesis is identical with that of this paper, namely, that the red cell may be treated as a liquid-filled elastic shell. In deciding how to analyze such a shell, they proposed to investigate which one of the following four theories should apply: (1) the liquid-interface theory, (2) the "membrane" theory, (3) the "pure bending" (inextensional bending) theory, (4) the complete shell theory. However, instead of developing a comprehensive theory meeting the requirements of theory 4 named above, and then specialize into the three successively simpler cases theories 3, 2, and 1, Rand and Burton dismissed the whole shell theory as "intractable", and introduced the following two equations as the basis for analysis:

$$P = T\left(\frac{1}{R_1} + \frac{1}{R_2}\right) \tag{B. 1}$$

$$P = S\left(\frac{1}{R_1} + \frac{1}{R_2}\right). \tag{B. 2}$$

The first equation (B.1) is addressed to membrane stretching. It states that a pressure differential P (dyne/cm^2) across a membrane is balanced by a tension T times the mean curvature of the surface. R_1, R_2 are the principal radii of curvature. The second equation (B.2) is supposed to account for the "resistance to bending." Here S is a parameter in units of dyne/cm, and is supposed to "include both rigidity and tension."

Now the first equation (B.1) is valid only if the principal tensions N_s, N_t (in our notation) are equal and equal to T. The second equation (B.2) is probably never valid. There is no theoretical basis for this equation. If it is valid for some special cases, the authors did not mention any.

Equation B.1 is applicable, of course, to a liquid interface, for which T stands for surface tension. For an elastic membrane it is true only in very special cases. The sphered red cell (analyzed in this paper) happens to be the one case in which $N_s = N_t$ and therefore Equation B.1 is applicable. For cells not in spherical shape, in general $N_s \neq N_t$ and Equation B.1 is not valid. For a cell membrane sucked into a pipette, whose diameter is smaller than the cell radius, Equation B.1 is definitely nonvalid. It is easy to see that $N_s \neq N_t$ at the mouth of the pipette.

Rand and Burton (18) stated that the Equations B.1 and B.2 must be validated by experiments. Unfortunately they used liquid droplets for this purpose. Since for liquid droplets Equation B.1 is unquestionably valid and Equation B.2 is irrelevant, the agreement between theory and experiment does not add new information. But no other justification was offered for applying the liquid-drop analysis to the red cell.

The method of analyzing the red cell employed by Rand and Burton is illustrated in Fig. 7 of their paper (18). The solid curve in that figure shows the length of the tongue of a red cell membrane sucked into a small pipette as a function of the pressure differential; the dotted curve shows what happens when a liquid drop was sucked by a small pipette. In the case of the liquid there is a critical pressure at which the liquid flows abruptly and entirely into the pipette. The same does not happen to the red cell. However, Rand and Burton identified on the solid curve a point called "critical" on the basis of a tendency for the cell membrane to vibrate at that pressure. This "critical" pressure is then considered to have the same meaning as the critical pressure of the liquid droplet. The conclusions drawn in reference (18) are based on such an identification.

Since neither the identification of the "critical" conditions, nor the critical pressure of the liquid droplet, has been shown to be applicable to the red cell membrane, the conclusions reached in reference (18) are not well founded, and further analysis will be needed to derive the full implications of the interesting and elegant experiments of Rand and Burton.

APPENDIX C

Justification for Neglecting the Effect of Bending on the Sphering Problem

Although a complete theory of bending is exceedingly complex, still we can obtain a simple estimate of the effect of bending on the sphering of red cells as follows. Note that the principal effect of bending on the equation of equilibium in the radial direction, Equation 2, is to add terms of the form $D\nabla^2 \cdot$ (change of curvature), where D is the bending rigidity $Eh^3/[12(1 - \nu^2)]$, and ∇^2 is the Laplacian operator. To estimate the magnitude of such a term, let us consider the polar region (dimple) of the red cell where the change of curvature is the largest. The mean curvature of the sphere is $1/a$, that of the initial dimple is of the order of $-1/a$. Therefore the change is of the order of $2/a$. This change occurs in a distance of

the order of a. Hence the bending term is of the order of $[Eh^3/12\,(1-\nu^2)]\,(2/a^3)$, which should be compared with the membrane-stress term N_s/a in Equation 2. Now for a conservative estimate let us ignore the surface tension, so that the membrane-stress term is $N_s^{(e)}/a$. Using Equations 8 a and 12, we obtain the result that in the equation for the radial equilibrium the ratio of the contribution from bending to that from stretching is of the order of

$$\frac{Eh^3}{12(1-\nu^2)}\,\frac{2}{a^3}\left[\frac{Ehe_s}{(1-\nu)a}\right]^{-1} = \frac{h^2}{12(1+\nu)a^2e_s}.$$

For the red blood cell, we have $h \doteq 10^{-6}$ cm, $a \doteq 4 \times 10^{-4}$ cm, $\nu \doteq 0.5$, and $e_s \doteq 0.2$ from Fig. 8; then the ratio named above becomes 1.74×10^{-6} to 1. Thus the effect of bending is quite negligible.

The equation of tangential equilibrium, Equation 1, is affected by bending through the transverse shear which is of the order of the gradient of the product of the bending rigidity D times the change of curvature. By an estimate similar to the above, we find that the ratio of the order of magnitude of the neglected term to those retained is also of the order of 10^{-6} to 1.

These estimates break down at the point on the red cell where the extensional strain e_s vanishes. At this point the membrane stress vanishes and the bending terms, though small, are all that is left in the equation. Thus there exists a narrow region, close to the equator of the red cell, in which bending predominates. To analyze the stresses in this narrow region we can use the "edge-layer" theory. The phenomenon of edge layer is well known in the theory of thin shells. It was first discovered by H. Reissner (19) in 1912 in his study of spherical domes resting on pillars. He showed that stresses in the domes are governed by the membrane equations except in a narrow region near the edges, where an adjustment to bending is necessary to satisfy the boundary conditions. The mathematical reason is very similar to the boundary-layer theory in fluid dynamics. The important fact is that the width of such an edge layer is of the order of the thickness of the shell. Related edge layers for plates and shells are discussed by Friedrichs (3) and by Fung and Wittrick (6).

Hence there is a narrow strip the width of which is comparable to the thickness of the cell membrane, i.e. of the order of several 100 A, located where $e_s = 0$, in which bending predominates. But the over-all effect of such a strip on the sphering of the entire cell is expected to be very small.

NOTATIONS

Capital letters refer to original shell. Lower cases to deformed shell.

In Text

a	radius of sphere; radius vector to point on meridian of sphered red cell
B	parameter defined in Equation 20
C_0, C_1, C_2	constants defining the shape of the relaxed red cell (see Equation 23)
E	an elastic modulus resembling the Young's modulus, a function of strain
e_s, e_t	components of Lagrangian or Green's strains (see Equation 6)
H, h	cell wall thickness before and after sphering
N_s, N_t	normal stress resultants in the meridional and latitudinal directions, respectively
p	internal pressure in the sphered red cell
r	radial distance from the axis of symmetry

R_1 , r_1	the radius of curvature of the meridian at P
R_2 , r_2	the orthogonal radius of curvature of the surface at P, equal to the distance from P to the intersection of the normal through P and the axis of symmetry
S, s	arc length measured from the pole to a point on the meridian
X, x	the distance of a point to the axis of symmetry
X_0	equatorial radius of relaxed red cell
Z, z	axial coordinate of point on surface
Θ, θ	angle of radius vectors ρ and a from center of red cell to a point on the meridian before and after sphering
λ_1 , λ_2	principal extension ratios (see Equation 5)
γ	surface tension in cell membrane
ν	Poisson's ratio
ρ	radius vector to point P on meridian of relaxed red cell
Φ, φ	the angle between the normal to a surface and the axis of symmetry

In Appendices

$\mathbf{e}(e_x , e_y , e_{xy})$	strain tensor and strain components respectively
e_1 , e_2	principal strains
g	gravitational acceleration
$\mathbf{I}$	Idemfactor, a diagonal matrix with elements = 1
S	a "bending" parameter introduced by Rand and Burton (18) (see Equation B.2)
T	surface tension
z	vertical distance from the free surface of water
α, β	strain invariants defined in Equation A.5
$\mu(\alpha, \beta)$, $\eta(\alpha, \beta)$, $\lambda(\alpha, \beta)$	elastic moduli defined by Equations A.9 and A.11
ρ	density of fluid outside droplet
$\bar{\rho}$	density of fluid in droplet
$\boldsymbol{\sigma}(\sigma_x , \sigma_y , \sigma_{xy})$	stress tensor and stress components respectively

REFERENCES

1. BAKER. R. F. 1964. *J. Ultrastruct. Res.* **11**:494.
2. FLÜGGE, W. 1964. Stresses in Shells. Springer-Verlag OHG, Berlin, W. Germany.
3. FRIEDRICHS, K. O. 1949. The Edge Effect in the Bending of Plates. Reissner Anniversary Volume: Contribution to Applied Mechanics. J. W. Edwards, editor. Ann Arbor, Michigan. See also *Proc. Symp. Appl. Math. Elasticity*. 1950. **3**.
4. FUNG, Y. C. 1966. *Federation Proc.* **25**(6):1761.
5. FUNG, Y. C. 1965. Foundations of Solid Mechanics. Prentice-Hall Inc., N. J.
6. FUNG, Y. C., and W. WITTRICK. 1955. *Quart. J. Mech. Appl. Math.* **8**:191.
7. GREEN, A. E. and J. E. ADKINS. 1960. Large Elastic Deformations and Nonlinear Continuum Mechanics. The Oxford University Press, London, Great Britain.
8. GREGERSON, M. I., C. A. BRYANT, W. E. HAMMERLE, S. USAMI, and S. CHIEN. 1967. *Science* **157**:825.
9. GUEST, M. M., T. P. BOND, R. G. COOPER, and J. R. DERRICK. 1963. *Science.* **142**:1319.
10. KOCHEN, J. A. 1966. Visco-elastic properties of the red cell membrane. *Proc. 1st Intern. Conf. Hemorheology*. Iceland. In press.
11. MCCUTCHEON, E. P., and R. F. RUSHMER. 1967. *Circulation Res.* **20**(2):149.

12. MICHAL, A. D. 1947. Matrix and Tensor Calculus. John Wiley & Sons Inc., N. Y.
13. MURPHY, J. R. 1965. *J. Lab. Clin. Med.* **65**(5):756.
14. PONDER, E. 1930. *Quart. J. Exptl. Physiol.* **20**:29.
15. PONDER, E. 1948. Hemolysis and Related Phenomena. New York. Grune & Stratton Inc., N. Y. Chap. 3.
16. PRAGER, W. 1945. *J. Appl. Phys.* **16**(12):837.
17. PRAGER, W. 1961. Introduction to Mechanics of Continua. Ginn and Co., Boston, Mass.
18. RAND, R. P., and A. C. BURTON. 1964. *Biophys. J.* **4**:115, 303.
19. REISSNER, H. 1912. Spannungen in Kugelschalen-(Kuppeln). Festschrift Mueller-Breslau, Leipzig, Germany.
20. STEWART, G. J. 1966. Ultrastructure of the human red cell integument. *Proc. 1st Intern. Conf. Hemorheology*. Iceland. In press.
21. TEITEL, P. 1965. *Nature.* **204**:409.